Peer-reviewed version available at *Nanomaterials* **2020**, *10*, 1833; doi:10.3390/nano10091833

Article

Exciton dynamics in droplet epitaxial quantum dots grown on (311)A oriented substrates

Marco Abbarchi [1,†,‡], Takaaki Mano[2,*] Takashi Kuroda [2,‡] and Kazuaki Sakoda[2,‡]

[1] Aix Marseille Univ, Universite de Toulon, CNRS, IM2NP, Marseille, France ;
[2] Research Center for Functional Materials, National Institute for Materials Science, 1-1 Namiki, Tsukuba, Ibaraki 305-0044.
* Correspondence: marco.abbarchi@im2np.fr

Abstract: Droplet epitaxy allows the efficient fabrication of a plethora of 3D, III-V-based nanostructures on different crystalline orientations. Quantum dots grown on (311)A-oriented surface are obtained with record surface density, with or without a wetting layer. These are appealing features for quantum-dot lasing, thanks to the large density of quantum emitters and a truly 3D lateral confinement. However, the intimate photophysics of this class of nanostructures has not yet been investigated. Here we address the main optical and electronic properties of s-shell excitons in individual quantum dots grown on (311)A substrates with photoluminescence spectroscopy experiments. We show the presence of neutral exciton and biexciton as well as positive and negative charged excitons. We investigate the origins of spectral broadening, identifying them in spectral diffusion at low temperature and phonon-interaction at higher temperature, the presence of fine interactions between electron and hole spin, and a relevant heavy-hole/light-hole mixing. We interpret the level filling with a simple Poissonian model reproducing the power excitation dependence of the s-shell excitons. These results are relevant for the further improvement of this class of quantum emitters and their exploitation as single photon sources for low density samples as well as for efficient lasers for high density samples.

Keywords: III-V Quantum dots, Droplet Epitaxy, exciton dynamics, (311)A oriented substrate

1. Introduction

The continuous development of droplet epitaxy (DE)[1–3] as growth protocol for III-V-based semiconductor nanostructures enabled the fabrication of state-of-the-art devices such as lasers[4–8] and quantum emitters, including single photon sources[9–13] and entangled photons[14–17] with electrical injection[18]. The versatility of this method allowed to grow many different semiconductor alloys (GaInSb[19], AlGaAs[20–24], InGaAs[25–31] InGaP[13,32,33]), forming a plethora of nanostructures[34] such as quantum dots (QDs), multiple-concentric quantum rings[5,10,35–40], coupled structures such as ring-on-a-disk[41], dot in-a-ring[42] or dot-on-a-disk[43], as well as elongated structures such as nanowires[7]. This technique allows to independently tune size and density of the nanostructures[44] and to grow them with or without a wetting layer[7,22,26,27,45–49], aspects that are not matched by the conventional Stranski-Krastanov approach based on strain[50].

Another aspect relevant for applications is the possibility to grow high-quality nanostructures on different substrate orientation, providing the ground for highly symmetric QDs on (111)A surfaces[13, 14,22,23,28,29,33,44,51–54] (e.g. for entangled photon pairs generation) and for ultra-high density quantum wires[7] and QDs[6,19,25,46–48,55,56] formation on the highly anisotropic (311)A surface (e.g. for laser emission). This latter class of nanostructures grown on (311)A surface has not yet been

thoroughly investigated and a clear assessment of the corresponding excitonic dynamics has not yet been reported.

In this paper we show a detailed structural and optical characterization of individual QDs grown on the (311)A surface. We provide a clear-cut attribution of the main recombination lines observed in the photoluminescence (PL) spectrum to the s-shell excitons[20,56,57] based on polarization resolved PL measurements, power dependence and line broadening measurements. Neutral exciton X and biexciton XX, positive X^+ and negative charged excitons X^- are characterised by the presence of fine interactions[20,21,27,58] as well as by heavy-hole/light-hole mixing[59–63]. Their power dependence under laser excitation above barrier is well reproduced by a simple Poissonian model that precisely accounts for the main features and allows to estimate the excitonic capture volume[64]. Inhomogeneous line broadening at low temperature is ascribed to spectral diffusion[11,17,65–68]induced by the presence of charged defects nearby the QDs[69] and is specific of the excitonic complex in study[70,71]. Finally, at larger temperature, the photoluminescence of individual QDs broadens and quenches owing to phonon interactions[72–74].

2. Materials and Methods

2.1. Sample fabrication

The sample was grown on a semi-insulating GaAs (311)A substrate by conventional solid-source molecular-beam epitaxy system. After the growth of a 2 μm-thick $Al_{0.55}Ga_{0.45}As$ layer, a 136 nm-thick $Al_{0.26}Ga_{0.74}As$ core-layer was grown at 610 °C. At the core-layer center GaAs QDs were formed by droplet epitaxy. On the $Al_{0.26}Ga_{0.74}As$ surface, nominally 1.5 monolayers of Ga (at a growth speed of about 0.1 monolayers per second) was supplied without As_4 flux at 275 °C for the droplets formation. These droplets were then crystallized into GaAs QDs by supplying an As_4 flux (2×10^{-6} Torr beam equivalent pressure) at 200 °C. The QDs were annealed at 400 °C for 10 min under As_4 flux supply without capping in order to improve the crystal quality. After annealing, the QDs were covered with a 30 nm-thick $Al_{0.26}Ga_{0.74}As$ capping layer at 400 °C and the rest of the $Al_{0.26}Ga_{0.74}As$ (38 nm) layer was grown at 625 °C. Once the entire growth sequence was completed, a rapid thermal annealing process was performed at 785 °C for 4 min in an As_4 atmosphere to improve the optical quality.

2.2. Optical spectroscopy

The photoluminescence (PL) of individual QDs was collected with a confocal-spectroscopic setup (lateral resolution about 1 μm) CW laser excitation was performed above-barrier, at 532 nm (about 2.3 eV). The PL is then fed into a spectrometer and detected by a Si-based CCD camera, allowing for a spectral resolution better than 50 μeV in full width at half maximum (FWHM). All experiments were performed in a liquid-helium cryostat between 10 and 100 K.

Peer-reviewed version available at Nanomaterials 2020, 10, 1833; doi:10.3390/nano10091833

3. Results and discussion

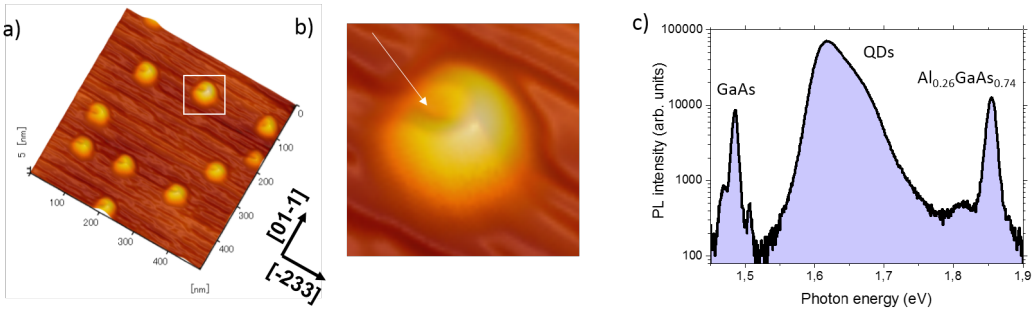

Figure 1. (**A**) Atomic force microscope micrograph representing a 3D view of GaAs QDs grown on a (311)A oriented $Al_{0.26}Ga_{0.74}As$ surface. The main chrstallographic axes are highlighted. (**B**) Blow-up of a single QD from **A**. The arrow highlights a hole in the QD side. (**C**) Photoluminescence (PL) spectrum (in semi-log scale) at 5 K showing the emission of (respectively from the low to the high energy side) the GaAs, the GaAs QDs and the $Al_{0.26}Ga_{0.74}As$ barrier layers.

Figure 1 A and B show atomic force micrographs (AFM) of the sample after annealing at 400 °C. Well-defined QDs are present with a density of about $5\times10^9/cm^2$. The QD morphology is highly asymmetric, with a U-shape (Figure 1 B). We attribute the formation mechanism of these asymmetric QDs to the low-intensity As_4 supply for the crystallization of the droplets and surface asymmetry of the (311)A surface[6,7,19,25,46–48,55]. In this growth conditions the Ga droplets crystallization into GaAs is enhanced around the edge of the droplets. In the case of standard (100) surface, in which the oppositely oriented directions of [011] and [0-11] are equivalent, ring-like structures with central holes are formed[35,36]. On the (311)A surface however, the oppositely oriented directions of [-233] and [2-3-3] are not equivalent while the directions of [01-1] and [0-11] are equivalent. Thus, the crystallization is enhanced only in a particular direction ([-233]). As the results, U-shaped QDs are formed.

Macro PL on the QDs ensemble taken at low temperature shows the different contributions from the GaAs substrate (at about 1.48 eV), the $Al_{0.26}Ga_{0.74}As$ barriers (at about 1.85 eV) and the QDs in between, extending over a broad band from about 1.55 eV up to 1.75 eV.

4. s-shell excitons.

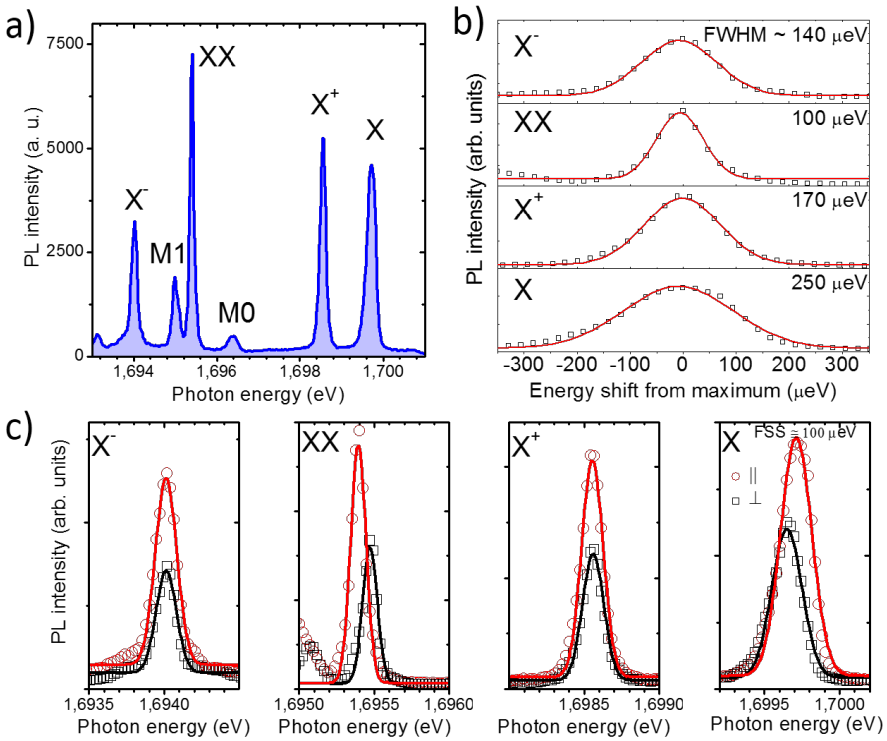

Figure 2. (**A**) PL spectrum of a single GaAs QD sandwiched between (311)A $Al_{0.35}Ga_{0.65}As$ barrier layers. The labels on the most intense lines X, X^+, XX and X^- highlight respectively the emission from the neutral exciton, the positive charged exciton, the neutral biexciton and the negative charged exciton. M0 and M1 highlight other non-attributed multiexciton complexes. (**B**) Symbols: PL spectra of X, X^+, XX and X^- (respectively from the bottom to the top panel). Red lines are Gaussian fit to the data. The corresponding full width at half maximum (FWHM) is reported on each panel. (**C**) Linearly polarized components of X, X^+, XX and X^- PL (respectively from the right to the left panel). Red and black symbols indicate orthogonal polarization. The continuous lines are Gaussians fits. The fine structure splitting (FSS) measured from the X and XX components, is about 100 μeV.

Typical spectra of individual QDs on (311)A substrate appear structured in several sharp lines (Figure 2 A). In analogy to most III-V epitaxial QDs including those fabricated via DE[9,20,75], in the low excitation power regime the s-shell excitons dominate the PL spectrum. We ascribe the brightest lines to the recombination of the neutral exciton X (one electron, *e*, and a heavy-hole, *hh*), neutral biexciton (XX, two *e* and two *hh*), positive charged exciton (one *e* and two *hh*), and to the negative charged exciton (two *e* and a *hh*). This attribution is based on the study of the electron-hole fine interaction[20] (fine structure splitting), line broadening[65] (spectral diffusion), and level filling[64], as discussed in the following sections. Seldom, we also observe other sharp lines, as M0 and M1 (Figure 2 A) that likely involve carrier recombination from the p-shell. However, a precise attribution of these lines is not possible with this set of data and goes beyond the aim of this paper.

4.1. e-h spin fine interaction: fine structure splitting.

A first identification of the s-shell excitons is based on the study of the fine interaction between electron and *hh* spin[20,21,58,76] (the fine structure splitting, FSS). At intermediate laser excitation power (at about 420 nW) all the PL components in the spectrum are well visible (Figure 2 A). At this power, by changing the polarization angle of the detected light we monitor the emission energy of the

PL. We observe for X and XX a mirror-symmetric energy splitting (Figure 2 C). X^+ and X^- instead, do not feature any splitting.

This picture corresponds very well to what is commonly observed in strain-free, III-V QDs: the presence of geometrical asymmetries in the confining potential breaks the invariance of the hamiltonian for rotations around the vertical growth axis[20,21,24,58,61,76,77]. More precisely, *e-h* spin-spin interaction for the X state lifts the degeneracy of the corresponding energy level and leads to two linearly polarised PL components depending on which recombination path is radiating. The XX state has overall zero spin for *e* and *hh* in the initial state and its FSS is completely determined by that of the X state, towards which it relaxes. X^+ and X^- can recombine with two possible energy equivalent paths and have no FSS.

The measured FSS in this QD is of about 100 μeV. In other QDs we measured values in between 30 and 140 μeV (not shown). These values are very large if compared with QDs grown on (111) substrates, where the three-fold symmetry of the crystal provides a more isotropic surface diffusion and a corresponding triangular or hexagonal nanostructure shape[13,14,22,23,28,29,33,44,51–54]. The origin of this splitting in (311)A QDs is attributed to asymmetries in the QDs shape that is affected by the anisotropy of the underlying crystal. The measured values of FSS are in line with those observed in (001) QDs in spite of the larger anisotropy of the (311)A surface[20,21,58,76]. Owing to the growth method in use, that allows for 3D growth of lattice-matched materials such as GaAs on AlGaAs, we exclude the presence of any strain in the structure that is a major origin of symmetry breaking (and thus FSS) in conventional Stranski-Krastanov III-V QDs[76].

4.2. Polarization intensity anisotropy: heavy-hole light-hole mixing.

A remarkable intensity change is visible for the two orthogonally polarized components (between 1/3 and 1/2, depending on the observed line, Figure 2 C)) of X and XX as well as in the polarization intensity of X^+ and X^-. We ascribe this difference to heavy-hole/light-hole (*hh-lh*) mixing[59–63,78]. This feature was first highlighted in DE QDs grown on (001)-oriented substrates and was explained as an effect of the different *hh* and *lh* bands dispersion in the different crystallographic directions[59]. While *e* states can be approximately described as isotropic and parabolic bands, valence *hh* and *lh* bands are affected by strong anisotropy and different curvatures. In spite of the large energy splitting between *hh* and *lh* bands in GaAs (tens of meV), strain and corresponding piezoelectricity[60,62,63,78] (in SK QDs) or shape asymmetries[59,61] (in DE QDs) lead to a substantial mixing of the corresponding *hh* and *lh* states, providing different selection rules (uneven PL intensity) for the two recombination paths. Here we observe differences in the PL intensity that are of the same order of those observed in the (001) counterpart[59,60,62,63,78].

5. Line broadening: spectral diffusion.

By monitoring the line-shape and corresponding broadening of each PL component in the s-shell we observe respectively, a common Gaussian envelope and a remarkably different full width at half maximum (FWHM, Figure 2 B). The common origin of the line broadening in this class of QDs is spectral diffusion: in spite of the expected natural linewidth that should be of the order of a few μeV with a corresponding Lorentian lineshape[65,67,68,75], the measured broadening values (tens to hundreds of μeV) and Gaussian envelopes are the fingerprints of a fluctuating charged environment. Charging and un-charging of electron and holes traps nearby the QDs (within a few tens of nm), produces a variable quantum confined Stark-shift of the excitonic energy levels[11,17,65–69]. A PL measurement lasting for a few seconds acquires many photons emitted at slightly different energy, thus providing a Gaussian lineshape. However, owing to the different *hh* and *e* confinement (larger penetration in the barrier for *e* with respect to *hh*) and a screening of external electric field for many-particles states, the corresponding Stark-shift can be very different. It has been rutinely reported a larger broadening of X with respect to the other s-shell excitons, whereas the relative broadening of XX, X^+ and X^- can be very different, depending on the carrier trapped and its position with respect to

the QD[11,65,79]. As an example, the case in Figure 2 B seems to correspond to electrons confined in the plane of the QD[65]. However, this picture can be quite different from a QD to another, owing to the randomness and local changes of the extrinsic disorder.

In this samples the presence of defects in the QDs environment is likely due to the rather low temperature used to form 3D nanostructures. This is a well-known issue affecting QDs grown by droplet epitaxy. However, in principle it could be overcome as it has been shown for droplet epitaxial QDs grown on other surface orientations[14,66].

6. Power dependence: level filling.

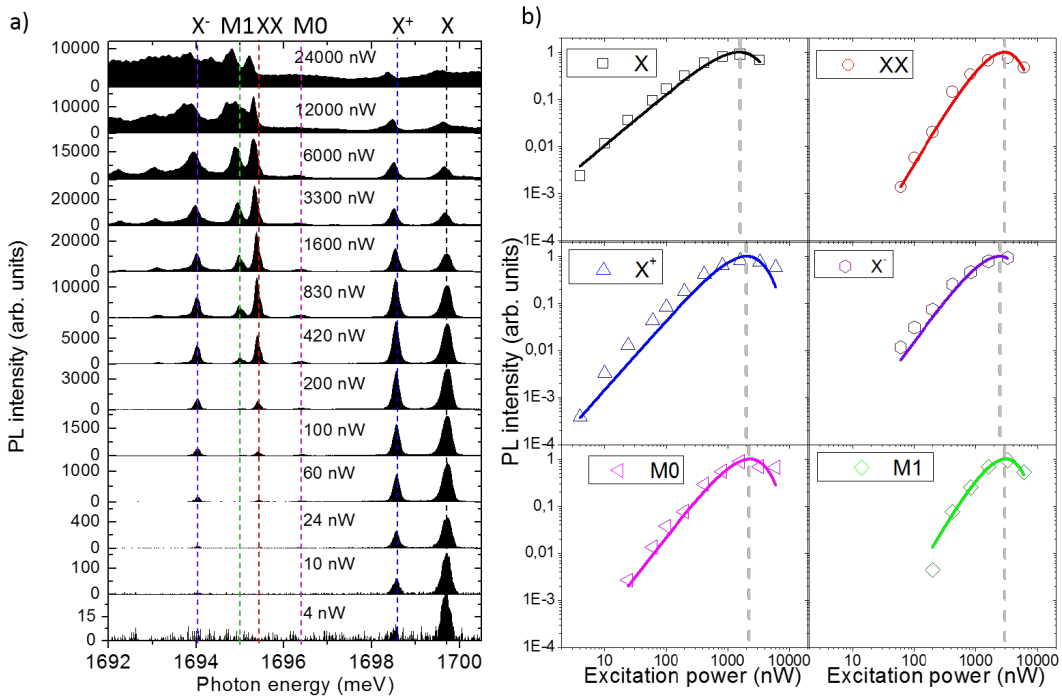

Figure 3. (**A**) PL spectra from low to high excitation power for the same QD shown in Fig. 2. The incident power is highlighted on each panel. The vertical dashed lines are guides to the eyes. (**B**) Evolution of the six main PL lines as a function of the incident excitation power. The PL intensity has been normalized to the maximum for each component. Each panel refers to a specific exciton complex recombination as highlighted by the corresponding labels. Symbols are the experimental data whereas lines are Poissonian fits.

A typical evolution of the PL spectrum of an individual QD as a function of the incident power is provided in Figure 3 A. At low power only two lines, X and X^+ are visible with a dominant intensity of X, while when increasing the power also X^- and, soon after, XX appear. At larger power X and X^+ swap their relative intensity and then quench. XX and X^- reach their maximum and quench at very large power. M0 and M1 follows a similar dynamics of X^- and XX, respectively. At lower energy, other peaks appear together with a broad background that then extends to all the spectrum. These latter features are interpreted as the effect of multi-excitons recombining from the p-shell and the coupling with the continuum of states above the confined energy levels. For the sake of thoroughness, we note a slight red-shift of the PL intensity at large excitation power. This effect is interpreted as a heating of the sample. It is also worth noting that the PL intensity of the s-shell excitons can be followed over more than 3 order of magnitude of the excitation power, meaning that the capture and recombination processes are very efficient in this sample.

A simple but meaningful description of the level filling of individual QDs can be provided by a model based on the assumption that carrier capture and recombination are random processes[80]. By assuming an infinite set of confined levels in the nanostructure, that obviously constitutes a rough approximation, the model can be further simplified to a Poissonian dependence of the PL intensity[64, 80]. In spite of its simplicity, this modeling accounts extremely well for power dependence[64] and recombination dynamics[33,81] of the s-shell excitons. In this model we assume that the PL intensity I_{PL} of a given energy level is proportional to the occupation probability N_n of that level:

$$I_{PL} \propto N_n \tag{1}$$

The Poissonian model for level filling predicts that the occupation of a certain level with n excitons N_n is provided by:

$$N_n = \frac{< n >^n}{n!} e^{-<n>} \tag{2}$$

Thus, for $n = 1$ N_1 describes the level filling of X, for $n = 2$ N_2 describes the level filling of XX, etc. $< n >$ is the average number of exciton created in the QD. This number is obtained averaging over many capture/recombination cycles and under steady state excitation and is defined as $< n >= N_R \tau_r / \tau_c$, with N_R is the number of e-h pairs created in the reservoir, τ_r is the exciton recombination rate and τ_c the exciton capture rate. Provided that τ_r and τ_c lie in the ps to ns range and the integration time for a PL measurement last about one second, this hypothesis is well satisfied.

A final phenomenological assumption for $< n >$ that allows to link the experimental data to this Poissonian model is that

$$< n >= \beta P_{exc}^{\alpha} \tag{3}$$

where α and β are constants characterising the capture mechanism. Note that in the vast majority of works on QDs, the level filling of the s-shell excitons is simply provided by equation 3, with $\alpha(X) \sim 1$ for X, and $\alpha(XX) \sim 2$ for XX. However, this over-simplified assumption does not account for saturation and quenching of the PL lines under CW excitation[18,20,52,82].

The Poissonian model well reproduces the power dependence of X and XX that are extracted by integrating in energy their PL line up to 1600 nW after background subtraction (3 B). Fitting the data using Equation 2 and 3 we obtain $\alpha_X = 1.1$ (very close to 1 as expected) and a simultaneous fit of X and XX with the same parameters. Saturation power of X is about 1500 nW and about two times larger for XX.

Although the simple Poissonian model allows only for neutral excitons capture ($n = 1, 2, ...$) and in principle cannot account for charged complexes, a nice fitting of the data can be recovered by assuming half-integer numbers[64]. In this case the model is modified by adding a phenomenological coefficient γ to α_X modifying as follows:

$$N_n = \frac{(< n >^n)^{\gamma}}{n!} e^{-<n>} \tag{4}$$

thus, for instance $\gamma = 1$ corresponds to the neutral exciton X state whereas $\gamma = 1.5$ is *one and an half exciton* (between X and XX), that is a charged exciton. By using Equation 4 we can nicely fit the power dependence of X^+ and X^- by keeping unchanged the parameters α and β that were used to fit X and XX (3 B). We obtain $\alpha(X^+) = 1.3\alpha(X)$ and $\alpha(X^-) = 1.6\alpha(X)$ that are very close to 1.5. Finally, we note that also the dynamics of M0 and M1 with incident power can be nicely accounted for by this pseudo-Poissonian model providing $\alpha(M0) = 1.5\alpha(X)$ and $\alpha(M1) = 2.1\alpha(X)$. These values of γ larger

than 1 account for the super-linear dependence on the incident power and suggest a multi-exciton nature of these energy levels.

To conclude this section we estimate the QD capture volume for excitons[64]. This can be deduced from the saturation power of the X level: at that power (of about 1500 nW distributed over a diameter of 1 μm) the number of carriers created in the host matrix around the QD provides a steady occupation of the X level by one exciton. Thus, the inverse of the carrier density injected in the semiconductor at that saturation power represents the capture volume. Assuming a penetration depth of the laser light of about 1 μm, an excitonic recombination lifetime of about 1 ns and considering the QD as a sphere, we can roughly deduce a capture radius of the order of 50 nm. This value is rather larger than the physical size of the QD, that is of the order of a few nm. We also observe that this value is perfectly in line with those measured in the (001) DE QDs counterpart[64] as well as in other kind of quantum emitters in III-V[79] and in group IV materials[83].

6.1. Temperature dependence.

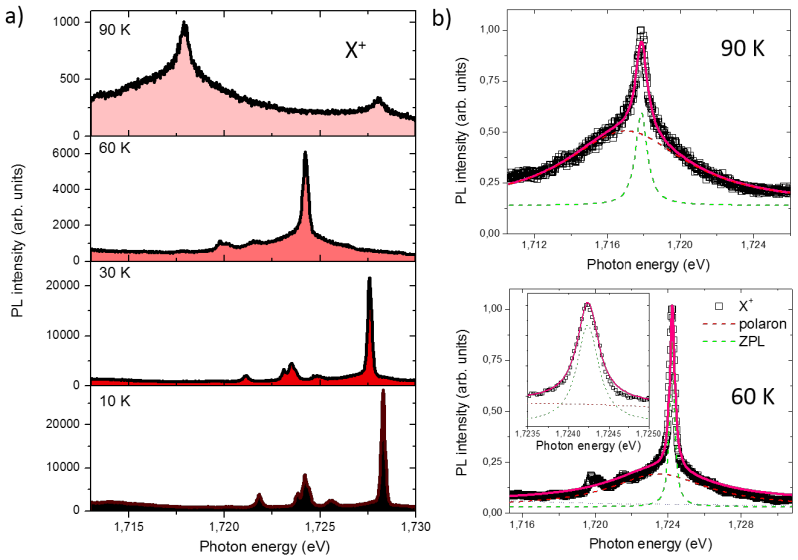

Figure 4. (**A**) Selected PL spectra from 10 to 90 K of a single QD with a bright X^+ emission. (**B**) Bottom panel: detail of the spectrum from A at 60 K with Lorentzian fits of the zero phonon line and the polaron band. The inset shows a blow up of the ZPL. Top panell: detail of the spectrum at 90 K with Lorentzian fits.

Bright PL emission can be observed well above liquid nitrogen temperature (Figure 4). A quadratic red-shift of the exciton emission is observed, as expected for this class of nanostructures that follows the empirical Varshini law (Figure 4 A). At the same time, a strong quenching of the PL intensity of about two orders of magnitude is observed when passing from 10 to 90 K.

The low-temperature spectrum (up to about 30 K), as discussed in the previous sections, shows sharp lines attributed to the s-shell excitons and is well described by a Gaussian envelope (Figure 2)[65]. At higher temperature instead, when the phonon population plays an important role, we observe the onset of a broad Lorentzian-shaped pedestal below the original sharp line that can be now well approximated with a Lorentzian envelope (Figure 4 B)[72,73,84]. The relative intensity of this broad pedestal increases up to dominate over the sharp central line. This phenomenology corresponds well to what has been thoroughly explained by using the Huang-Rhys formalism for (001) DE QDs as well as for SK QDs[72,73,84]: the broad band is interpreted as a superposition of acoustic phonon replicas (polaron) whereas the sharp central line emission is assigned to the zero phonon line (ZPL).

7. Conclusions

In conclusion we showed that droplet epitaxial QDs grown on the highly anisotropic (311)A surface are characterised by bright PL lines emitting at visible frequency. These lines correspond well to the picture of s-shell excitons recombination in III-V nanostructures. We measured a relatively large fine structure splitting (10-100 μeV) of the neutral exciton X, that is justified by the anisotropic shape of these QDs. Inhomogeneus line broadening lies in the 100μeV and is ascribed to spectral diffusion originating from the fluctuating charged environment. This broadening is specific of each excitonic species and reflects the nature and position of the trapped carriers. Level filling of the s-shell excitons is well accounted for by a simple Poissonian model that allows to describe the power dependence of the main PL lines and to estimate an excitonic capture volume much larger than the physical size of the QD. Finally, a bright PL emission is still visible well above liquid nitrogen temperature.

Overall, these results account for the high quality and brightness of this class of QDs where X, XX and X^+ emission can be followed for about 3 orders of magnitude of excitation power below saturation and up to relatively large temperature that are appealing features for applications as single photon sources. The low-temperature linewidth is rather large with respect to state-of-the-art droplet epitaxial quantum dots and in principle it could be improved by using alternative fabrication processes at higher temperature.

Funding:

Acknowledgments:

Conflicts of Interest: The authors declare no conflict of interest.

Abbreviations

The following abbreviations are used in this manuscript:

PL	photoluminescence
QD	quantum dot
FSS	fine structure splitting
X	neutral exciton
X^+	positive charged exciton
XX	neutral biexciton
X^-	negative charged exciton
FWHM	full width at half maximum

1. Mantovani, V.; Sanguinetti, S.; Guzzi, M.; Grilli, E.; Gurioli, M.; Watanabe, K.; Koguchi, N. Low density GaAs/ AlGaAs quantum dots grown by modified droplet epitaxy. *Journal of applied physics* **2004**, *96*, 4416–4420.
2. Wu, J.; Wang, Z.M. Droplet epitaxy for advanced optoelectronic materials and devices. *Journal of Physics D: Applied Physics* **2014**, *47*, 173001.
3. Gurioli, M.; Wang, Z.; Rastelli, A.; Kuroda, T.; Sanguinetti, S. Droplet epitaxy of semiconductor nanostructures for quantum photonic devices. *Nature materials* **2019**, p. 1.
4. Mano, T.; Kuroda, T.; Yamagiwa, M.; Kido, G.; Sakoda, K.; Koguchi, N. Lasing in Ga As/ Al Ga As self-assembled quantum dots. *Applied physics letters* **2006**, *89*, 183102.
5. Mano, T.; Kuroda, T.; Mitsuishi, K.; Yamagiwa, M.; Guo, X.J.; Furuya, K.; Sakoda, K.; Koguchi, N. Ring-shaped GaAs quantum dot laser grown by droplet epitaxy: effects of post-growth annealing on structural and optical properties. *Journal of crystal growth* **2007**, *301*, 740–743.
6. Mano, T.; Kuroda, T.; Mitsuishi, K.; Nakayama, Y.; Noda, T.; Sakoda, K. Ga As/ Al Ga As quantum dot laser fabricated on GaAs (311) A substrate by droplet epitaxy. *Applied Physics Letters* **2008**, *93*, 203110.
7. Jo, M.; Keizer, J.G.; Mano, T.; Koenraad, P.M.; Sakoda, K. Self-assembly of GaAs quantum wires grown on (311) A substrates by droplet epitaxy. *Applied physics express* **2011**, *4*, 055501.

8. Jo, M.; Mano, T.; Sakoda, K. Electrical Lasing in GaAs Quantum Dots Grown by Droplet Epitaxy. Advances in Optical Materials. Optical Society of America, 2012, pp. ITh5B–6.
9. Kuroda, T.; Abbarchi, M.; Mano, T.; Watanabe, K.; Yamagiwa, M.; Kuroda, K.; Sakoda, K.; Kido, G.; Koguchi, N.; Mastrandrea, C.; others. Photon correlation in GaAs self-assembled quantum dots. *Applied physics express* **2008**, *1*, 042001.
10. Abbarchi, M.; Mastrandrea, C.; Vinattieri, A.; Sanguinetti, S.; Mano, T.; Kuroda, T.; Koguchi, N.; Sakoda, K.; Gurioli, M. Photon antibunching in double quantum ring structures. *Physical Review B* **2009**, *79*, 085308.
11. Abbarchi, M.; Kuroda, T.; Mano, T.; Gurioli, M.; Sakoda, K. Bunched photon statistics of the spectrally diffusive photoluminescence of single self-assembled GaAs quantum dots. *Physical Review B* **2012**, *86*, 115330.
12. Benyoucef, M.; Zuerbig, V.; Reithmaier, J.P.; Kroh, T.; Schell, A.W.; Aichele, T.; Benson, O. Single-photon emission from single InGaAs/GaAs quantum dots grown by droplet epitaxy at high substrate temperature. *Nanoscale research letters* **2012**, *7*, 1–5.
13. Kumano, H.; Harada, T.; Suemune, I.; Nakajima, H.; Kuroda, T.; Mano, T.; Sakoda, K.; Odashima, S.; Sasakura, H. Stable and efficient collection of single photons emitted from a semiconductor quantum dot into a single-mode optical fiber. *Applied Physics Express* **2016**, *9*, 032801.
14. Kuroda, T.; Mano, T.; Ha, N.; Nakajima, H.; Kumano, H.; Urbaszek, B.; Jo, M.; Abbarchi, M.; Sakuma, Y.; Sakoda, K.; others. Symmetric quantum dots as efficient sources of highly entangled photons: Violation of Bell's inequality without spectral and temporal filtering. *Physical Review B* **2013**, *88*, 041306.
15. Kumano, H.; Nakajima, H.; Kuroda, T.; Mano, T.; Sakoda, K.; Suemune, I. Nonlocal biphoton generation in a Werner state from a single semiconductor quantum dot. *Physical review B* **2015**, *91*, 205437.
16. Basso Basset, F.; Bietti, S.; Reindl, M.; Esposito, L.; Fedorov, A.; Huber, D.; Rastelli, A.; Bonera, E.; Trotta, R.; Sanguinetti, S. High-yield fabrication of entangled photon emitters for hybrid quantum networking using high-temperature droplet epitaxy. *Nano letters* **2018**, *18*, 505–512.
17. Ramírez, H.Y.; Chou, Y.L.; Cheng, S.J. Effects of electrostatic environment on the electrically triggered production of entangled photon pairs from droplet epitaxial quantum dots. *Scientific reports* **2019**, *9*, 1–10.
18. Ha, N.; Mano, T.; Kuroda, T.; Sakuma, Y.; Sakoda, K. Current-injection quantum-entangled-pair emitter using droplet epitaxial quantum dots on GaAs (111) A. *Applied Physics Letters* **2019**, *115*, 083106.
19. Kawazu, T.; Noda, T.; Mano, T.; Jo, M.; Sakaki, H. Effects of antimony flux on morphology and photoluminescence spectra of GaSb quantum dots formed on GaAs by droplet epitaxy. *Journal of Nonlinear Optical Physics & Materials* **2010**, *19*, 819–826.
20. Abbarchi, M.; Mastrandrea, C.; Kuroda, T.; Mano, T.; Sakoda, K.; Koguchi, N.; Sanguinetti, S.; Vinattieri, A.; Gurioli, M. Exciton fine structure in strain-free GaAs/Al 0.3 Ga 0.7 As quantum dots: Extrinsic effects. *Physical Review B* **2008**, *78*, 125321.
21. Plumhof, J.; Křápek, V.; Wang, L.; Schliwa, A.; Bimberg, D.; Rastelli, A.; Schmidt, O. Experimental investigation and modeling of the fine structure splitting of neutral excitons in strain-free GaAs/Al x Ga 1-x As quantum dots. *Physical Review B* **2010**, *81*, 121309.
22. Mano, T.; Abbarchi, M.; Kuroda, T.; McSkimming, B.; Ohtake, A.; Mitsuishi, K.; Sakoda, K. Self-assembly of symmetric GaAs quantum dots on (111) A substrates: Suppression of fine-structure splitting. *Applied physics express* **2010**, *3*, 065203.
23. Bouet, L.; Vidal, M.; Mano, T.; Ha, N.; Kuroda, T.; Durnev, M.; Glazov, M.; Ivchenko, E.; Marie, X.; Amand, T.; others. Charge tuning in [111] grown GaAs droplet quantum dots. *Applied Physics Letters* **2014**, *105*, 082111.
24. Yeo, I.; Kim, D.; Lee, K.T.; Kim, J.S.; Song, J.D.; Park, C.H.; Han, I.K. Comparative Chemico-Physical Analyses of Strain-Free GaAs/Al0. 3Ga0. 7As Quantum Dots Grown by Droplet Epitaxy. *Nanomaterials* **2020**, *10*, 1301.
25. Saidi, F.; Bouzaiene, L.; Sfaxi, L.; Maaref, H. Growth conditions effects on optical properties of InAs quantum dots grown by molecular beam epitaxy on GaAs (1 1 3) A substrate. *Journal of luminescence* **2012**, *132*, 289–292.
26. Zuerbig, V.; Bugaew, N.; Reithmaier, J.P.; Kozub, M.; Musiał, A.; Sęk, G.; Misiewicz, J. Growth-Temperature Dependence of Wetting Layer Formation in High Density InGaAs/GaAs Quantum Dot Structures Grown by Droplet Epitaxy. *Japanese Journal of Applied Physics* **2012**, *51*, 085501.

27. Skiba-Szymanska, J.; Stevenson, R.M.; Varnava, C.; Felle, M.; Huwer, J.; Müller, T.; Bennett, A.J.; Lee, J.P.; Farrer, I.; Krysa, A.B.; others. Universal growth scheme for quantum dots with low fine-structure splitting at various emission wavelengths. *Physical Review Applied* **2017**, *8*, 014013.
28. Mano, T.; Mitsuishi, K.; Ha, N.; Ohtake, A.; Castellano, A.; Sanguinetti, S.; Noda, T.; Sakuma, Y.; Kuroda, T.; Sakoda, K. Growth of metamorphic InGaAs on GaAs (111) a: counteracting lattice mismatch by inserting a thin InAs interlayer. *Crystal Growth & Design* **2016**, *16*, 5412–5417.
29. Ha, N.; Mano, T.; Wu, Y.N.; Ou, Y.W.; Cheng, S.J.; Sakuma, Y.; Sakoda, K.; Kuroda, T. Wavelength extension beyond 1.5 μm in symmetric InAs quantum dots grown on InP (111) A using droplet epitaxy. *Applied Physics Express* **2016**, *9*, 101201.
30. Fuster, D.; Abderrafi, K.; Alén, B.; González, Y.; Wewior, L.; González, L. InAs nanostructures grown by droplet epitaxy directly on InP (001) substrates. *Journal of Crystal Growth* **2016**, *434*, 81–87.
31. Sala, E.M.; Na, Y.I.; Godsland, M.; Trapalis, A.; Heffernan, J. InAs/InP Quantum Dots in Etched Pits by Droplet Epitaxy in Metalorganic Vapor Phase Epitaxy. *physica status solidi (RRL) – Rapid Research Letters* **2020**, *n/a*, 2000173, [https://onlinelibrary.wiley.com/doi/pdf/10.1002/pssr.202000173]. doi:10.1002/pssr.202000173.
32. Prongjit, P.; Ratanathammaphan, S.; Ha, N.; Mano, T.; Sakoda, K.; Kuroda, T. Type-II recombination dynamics of tensile-strained GaP quantum dots in GaAs grown by droplet epitaxy. *Applied Physics Letters* **2016**, *109*, 171902.
33. Ha, N.; Mano, T.; Dubos, S.; Kuroda, T.; Sakuma, Y.; Sakoda, K. Single photon emission from droplet epitaxial quantum dots in the standard telecom window around a wavelength of 1.55 μm. *Applied Physics Express* **2020**, *13*, 025002.
34. Bietti, S.; Bocquel, J.; Adorno, S.; Mano, T.; Keizer, J.G.; Koenraad, P.M.; Sanguinetti, S. Precise shape engineering of epitaxial quantum dots by growth kinetics. *Physical Review B* **2015**, *92*, 075425.
35. Mano, T.; Koguchi, N. Nanometer-scale GaAs ring structure grown by droplet epitaxy. *Journal of crystal growth* **2005**, *278*, 108–112.
36. Mano, T.; Kuroda, T.; Sanguinetti, S.; Ochiai, T.; Tateno, T.; Kim, J.; Noda, T.; Kawabe, M.; Sakoda, K.; Kido, G.; others. Self-assembly of concentric quantum double rings. *Nano letters* **2005**, *5*, 425–428.
37. Somaschini, C.; Bietti, S.; Koguchi, N.; Sanguinetti, S. Fabrication of multiple concentric nanoring structures. *Nano letters* **2009**, *9*, 3419–3424.
38. Shwartz, N.L.; Vasilenko, M.A.; Nastovjak, A.G.; Neizvestny, I.G. Concentric GaAs nanorings formation by droplet epitaxy—Monte Carlo simulation. *Computational Materials Science* **2018**, *141*, 91–100.
39. Sanguinetti, S.; Mano, T.; Kuroda, T. Self-assembled semiconductor quantum ring complexes by droplet epitaxy: growth and physical properties. In *Physics of Quantum Rings*; Springer, 2018; pp. 187–228.
40. Heyn, C.; Zocher, M.; Hansen, W. Functionalization of Droplet Etching for Quantum Rings. In *Physics of Quantum Rings*; Springer, 2018; pp. 139–162.
41. Somaschini, C.; Bietti, S.; Sanguinetti, S.; Koguchi, N.; Fedorov, A. Self-assembled GaAs/AlGaAs coupled quantum ring-disk structures by droplet epitaxy. *Nanotechnology* **2010**, *21*, 125601.
42. Somaschini, C.; Bietti, S.; Koguchi, N.; Sanguinetti, S. Coupled quantum dot–ring structures by droplet epitaxy. *Nanotechnology* **2011**, *22*, 185602.
43. Elborg, M.; Noda, T.; Mano, T.; Kuroda, T.; Yao, Y.; Sakuma, Y.; Sakoda, K. Self-assembly of vertically aligned quantum ring-dot structure by Multiple Droplet Epitaxy. *Journal of Crystal Growth* **2017**, *477*, 239–242.
44. Ohtake, A.; Ha, N.; Mano, T. Extremely high-and low-density of Ga droplets on GaAs {111} A, B: Surface-polarity dependence. *Crystal Growth & Design* **2015**, *15*, 485–488.
45. Sanguinetti, S.; Watanabe, K.; Tateno, T.; Wakaki, M.; Koguchi, N.; Kuroda, T.; Minami, F.; Gurioli, M. Role of the wetting layer in the carrier relaxation in quantum dots. *Applied physics letters* **2002**, *81*, 613–615.
46. Mano, T.; Noda, T.; Kuroda, T.; Sanguinetti, S.; Sakoda, K. Self-assembled GaAs quantum dots coupled with GaAs wetting layer grown on GaAs (311) A by droplet epitaxy. *physica status solidi c* **2011**, *8*, 257–259.
47. Keizer, J.; Jo, M.; Mano, T.; Noda, T.; Sakoda, K.; Koenraad, P. Structural atomic-scale analysis of GaAs/AlGaAs quantum wires and quantum dots grown by droplet epitaxy on a (311) A substrate. *Applied Physics Letters* **2011**, *98*, 193112.

48. Keizer, J.; Koenraad, P. Atomic-scale analysis of self-assembled quantum dots by cross-sectionalscanning, tunneling microscopy, and atom probe tomography. In *Quantum Dots: Optics, Electron Transport and Future Applications*; Cambridge University Press, 2012; pp. 41–60.
49. Shahzadeh, M.; Sabaeian, M. Wetting layer-assisted modification of in-plane-polarized transitions in strain-free GaAs/AlGaAs quantum dots. *Superlattices and Microstructures* **2014**, *75*, 514–522.
50. Sautter, K.E.; Vallejo, K.D.; Simmonds, P.J. Strain-driven quantum dot self-assembly by molecular beam epitaxy. *Journal of Applied Physics* **2020**, *128*, 031101.
51. Jo, M.; Mano, T.; Abbarchi, M.; Kuroda, T.; Sakuma, Y.; Sakoda, K. Self-limiting growth of hexagonal and triangular quantum dots on (111) A. *Crystal growth & design* **2012**, *12*, 1411–1415.
52. Liu, X.; Ha, N.; Nakajima, H.; Mano, T.; Kuroda, T.; Urbaszek, B.; Kumano, H.; Suemune, I.; Sakuma, Y.; Sakoda, K. Vanishing fine-structure splittings in telecommunication-wavelength quantum dots grown on (111) A surfaces by droplet epitaxy. *Physical Review B* **2014**, *90*, 081301.
53. Trapp, A.; Reuter, D. Formation of self-assembled GaAs quantum dots via droplet epitaxy on misoriented GaAs (111) B substrates. *Journal of Vacuum Science & Technology B, Nanotechnology and Microelectronics: Materials, Processing, Measurement, and Phenomena* **2018**, *36*, 02D106.
54. Bietti, S.; Basset, F.B.; Tuktamyshev, A.; Bonera, E.; Fedorov, A.; Sanguinetti, S. High–temperature droplet epitaxy of symmetric GaAs/AlGaAs quantum dots. *Scientific Reports* **2020**, *10*, 1–10.
55. Mano, T.; Kuroda, T.; Mitsuishi, K.; Noda, T.; Sakoda, K. High-density GaAs/AlGaAs quantum dots formed on GaAs (3 1 1) A substrates by droplet epitaxy. *Journal of crystal growth* **2009**, *311*, 1828–1831.
56. Abbarchi, M.; Kuroda, T.; Mano, T.; Sakoda, K.; Mastrandrea, C.A.; Vinattieri, A.; Gurioli, M.; Tsuchiya, T. Energy renormalization of exciton complexes in GaAs quantum dots. *Physical Review B* **2010**, *82*, 201301.
57. Accanto, N.; Minari, S.; Cavigli, L.; Bietti, S.; Isella, G.; Vinattieri, A.; Sanguinetti, S.; Gurioli, M. Kinetics of multiexciton complex in gaas quantum dots on si. *Applied Physics Letters* **2013**, *102*, 053109.
58. Tong, H.; Wu, M. Theory of excitons in cubic III-V semiconductor GaAs, InAs and GaN quantum dots: fine structure and spin relaxation. *Physical Review B* **2011**, *83*, 235323.
59. Belhadj, T.; Amand, T.; Kunold, A.; Simon, C.M.; Kuroda, T.; Abbarchi, M.; Mano, T.; Sakoda, K.; Kunz, S.; Marie, X.; others. Impact of heavy hole-light hole coupling on optical selection rules in GaAs quantum dots. *Applied Physics Letters* **2010**, *97*, 051111.
60. Lin, C.H.; You, W.T.; Chou, H.Y.; Cheng, S.J.; Lin, S.D.; Chang, W.H. Anticorrelation between the splitting and polarization of the exciton fine structure in single self-assembled InAs/GaAs quantum dots. *Physical Review B* **2011**, *83*, 075317.
61. Liao, Y.H.; Liao, C.C.; Ku, C.H.; Chang, Y.C.; Cheng, S.J.; Jo, M.; Kuroda, T.; Mano, T.; Abbarchi, M.; Sakoda, K. Geometrical impact on the optical polarization of droplet epitaxial quantum dots. *Physical Review B* **2012**, *86*, 115323.
62. Plumhof, J.; Trotta, R.; Křápek, V.; Zallo, E.; Atkinson, P.; Kumar, S.; Rastelli, A.; Schmidt, O.G. Tuning of the valence band mixing of excitons confined in GaAs/AlGaAs quantum dots via piezoelectric-induced anisotropic strain. *Physical Review B* **2013**, *87*, 075311.
63. Luo, J.W.; Bester, G.; Zunger, A. Supercoupling between heavy-hole and light-hole states in nanostructures. *Physical Review B* **2015**, *92*, 165301.
64. Abbarchi, M.; Mastrandrea, C.; Kuroda, T.; Mano, T.; Vinattieri, A.; Sakoda, K.; Gurioli, M. Poissonian statistics of excitonic complexes in quantum dots. *Journal of Applied Physics* **2009**, *106*, 053504.
65. Abbarchi, M.; Troiani, F.; Mastrandrea, C.; Goldoni, G.; Kuroda, T.; Mano, T.; Sakoda, K.; Koguchi, N.; Sanguinetti, S.; Vinattieri, A.; others. Spectral diffusion and line broadening in single self-assembled Ga As/ Al Ga As quantum dot photoluminescence. *Applied physics letters* **2008**, *93*, 162101.
66. Mano, T.; Abbarchi, M.; Kuroda, T.; Mastrandrea, C.; Vinattieri, A.; Sanguinetti, S.; Sakoda, K.; Gurioli, M. Ultra-narrow emission from single GaAs self-assembled quantum dots grown by droplet epitaxy. *Nanotechnology* **2009**, *20*, 395601.
67. Kuroda, K.; Kuroda, T.; Watanabe, K.; Mano, T.; Kido, G.; Koguchi, N.; Sakoda, K. Distribution of exciton emission linewidth observed for GaAs quantum dots grown by droplet epitaxy. *Journal of luminescence* **2010**, *130*, 2390–2393.
68. Nguyen, H.S.; Sallen, G.; Abbarchi, M.; Ferreira, R.; Voisin, C.; Roussignol, P.; Cassabois, G.; Diederichs, C. Photoneutralization and slow capture of carriers in quantum dots probed by resonant excitation spectroscopy. *Physical review B* **2013**, *87*, 115305.

69. Ha, N.; Mano, T.; Chou, Y.L.; Wu, Y.N.; Cheng, S.J.; Bocquel, J.; Koenraad, P.M.; Ohtake, A.; Sakuma, Y.; Sakoda, K.; others. Size-dependent line broadening in the emission spectra of single GaAs quantum dots: Impact of surface charge on spectral diffusion. *Physical Review B* **2015**, *92*, 075306.
70. Schimpf, C.; Reindl, M.; Klenovskỳ, P.; Fromherz, T.; Da Silva, S.F.C.; Hofer, J.; Schneider, C.; Höfling, S.; Trotta, R.; Rastelli, A. Resolving the temporal evolution of line broadening in single quantum emitters. *Optics Express* **2019**, *27*, 35290–35307.
71. Reigue, A.; Hostein, R.; Voliotis, V. Resonance fluorescence of a single semiconductor quantum dot: the impact of a fluctuating electrostatic environment. *Semiconductor Science and Technology* **2019**, *34*, 113001.
72. Sanguinetti, S.; Mano, T.; Oshima, M.; Tateno, T.; Wakaki, M.; Koguchi, N. Temperature dependence of the photoluminescence of InGaAs/GaAs quantum dot structures without wetting layer. *Applied physics letters* **2002**, *81*, 3067–3069.
73. Abbarchi, M.; Gurioli, M.; Vinattieri, A.; Sanguinetti, S.; Bonfanti, M.; Mano, T.; Watanabe, K.; Kuroda, T.; Koguchi, N. Phonon sideband recombination kinetics in single quantum dots. *Journal of applied physics* **2008**, *104*, 023504.
74. Lee, S.e.; Yeo, I.; Jo, M.K.; Jeong, Y.W.; Kim, T.G.; Kim, J.S.; Yi, K.S.; Han, I.K.; Song, J.D. Exciton-phonon coupling channels in a 'strain-free'GaAs droplet epitaxy single quantum dot. *Current Applied Physics* **2018**, *18*, 829–833.
75. Abbarchi, M.; Kuroda, T.; Duval, R.; Mano, T.; Sakoda, K. Scanning Fabry-Pérot interferometer with largely tuneable free spectral range for high resolution spectroscopy of single quantum dots. *Review of Scientific Instruments* **2011**, *82*, 073103.
76. Trotta, R.; Zallo, E.; Ortix, C.; Atkinson, P.; Plumhof, J.; Van den Brink, J.; Rastelli, A.; Schmidt, O. Universal recovery of the energy-level degeneracy of bright excitons in InGaAs quantum dots without a structure symmetry. *Physical review letters* **2012**, *109*, 147401.
77. Adorno, S.; Bietti, S.; Sanguinetti, S. Annealing induced anisotropy in GaAs/AlGaAs quantum dots grown by droplet epitaxy. *Journal of crystal growth* **2013**, *378*, 515–518.
78. Fras, F.; Bernardot, F.; Eble, B.; Bernard, M.; Siarry, B.; Miard, A.; Lemaitre, A.; Testelin, C.; Chamarro, M. The role of heavy–light-hole mixing on the optical initialization of hole spin in InAs quantum dots. *Journal of Physics: Condensed Matter* **2013**, *25*, 202202.
79. Dotti, N.; Sarti, F.; Bietti, S.; Azarov, A.; Kuznetsov, A.; Biccari, F.; Vinattieri, A.; Sanguinetti, S.; Abbarchi, M.; Gurioli, M. Germanium-based quantum emitters towards a time-reordering entanglement scheme with degenerate exciton and biexciton states. *Physical Review B* **2015**, *91*, 205316.
80. Grundmann, M.; Bimberg, D. Theory of random population for quantum dots. *Physical Review B* **1997**, *55*, 9740.
81. Kuroda, T.; Belhadj, T.; Abbarchi, M.; Mastrandrea, C.; Gurioli, M.; Mano, T.; Ikeda, N.; Sugimoto, Y.; Asakawa, K.; Koguchi, N.; others. Bunching visibility for correlated photons from single GaAs quantum dots. *Physical Review B* **2009**, *79*, 035330.
82. Tighineanu, P.; Daveau, R.; Lee, E.H.; Song, J.D.; Stobbe, S.; Lodahl, P. Decay dynamics and exciton localization in large GaAs quantum dots grown by droplet epitaxy. *Physical Review B* **2013**, *88*, 155320.
83. Beaufils, C.; Redjem, W.; Rousseau, E.; Jacques, V.; Kuznetsov, A.Y.; Raynaud, C.; Voisin, C.; Benali, A.; Herzig, T.; Pezzagna, S.; others. Optical properties of an ensemble of G-centers in silicon. *Physical Review B* **2018**, *97*, 035303.
84. Favero, I.; Cassabois, G.; Ferreira, R.; Darson, D.; Voisin, C.; Tignon, J.; Delalande, C.; Bastard, G.; Roussignol, P.; Gérard, J. Acoustic phonon sidebands in the emission line of single InAs/GaAs quantum dots. *Physical Review B* **2003**, *68*, 233301.